Electrode Independent Chemoresistive Response for Cobalt Phthalocyanine in the Space Charge Limited Conductivity Regime

Karla A. Miller,[†] Richard D. Yang,[†,§] Michael J. Hale,[†] Jeongwon Park,[§] Bernd Fruhberger,[‡] Corneliu N. Colesniuc,[‡] Ivan K. Schuller,[‡] Andrew C. Kummel,*,[†,⊥] and William C. Trogler*,[†,∥]

Department of Chemistry and Biochemistry, Materials Science and Engineering Program, and Department of Physics, University of California, San Diego, 9500 Gilman Drive, La Jolla, California 92093

Received: June 9, 2005; In Final Form: July 29, 2005

The electrical properties of 50 nm thick metallophthalocyanine films, prepared by organic molecular beam epitaxy (OMBE) on interdigitated electrodes, were studied with DC current−voltage measurements and impedance spectroscopy. The transition from Ohmic behavior at low voltages to space-charge-limited conductivity (SCLC) at higher voltages depends on the metal electrode (Pt, Pd, and Au), but does not correlate with the work function of the electrode. Impedance spectroscopy studies show the coexistence of low- and high-frequency traps in the thin film devices, and the contribution of low-frequency traps associated with Ohmic behavior diminishes at higher bias. Although device resistances are strongly influenced by the electrode material, and vary by a factor of over 300, the relative chemical sensor responses on exposure to dimethyl methylphosphonate (DMMP), methanol, water, or toluene vapors are similar for CoPc on Pt, Pd, and Au electrodes when these devices are operated in the SCLC regime at room temperature. When the devices are operated at voltages where the low-frequency interfacial traps are filled, the sensor response to analyte becomes uniform and reliable regardless of the specific interfacial electrode contact.

Introduction

Charge transport in organic materials is an important basic research topic that is relevant to device applications of organic semiconductors. Metallophthalocyanines (MPc) have been used as model systems for conduction in organic materials because they are chemically stable and can be readily deposited in a vacuum.[1,2] They have several technological applications,[3] such as charge transport layers in organic light emitting diodes (OLED)[4] and thin film transistors.[5] Electrical properties of the MPcs can be tuned by varying both the metal centers and peripheral organic substituents. Electrical conductivity measurements have been systematically performed on MPc thin films for thicknesses between 0.1 and 20 μm.[6−13] It has been found that the conductivity is dominated either by thermally generated or electrode-injected carriers.[9] At low field, the primary conduction behavior is Ohmic, as thermally generated carriers and carriers created by oxidation from atmospheric oxygen[14,15] exceed those of electrode injected carriers. At high field, space-charge-limited conductivity (SCLC) dominates as electrode-injected carriers exceed the thermally generated ones in the film. Previous studies of undoped ZnPc films 20 nm thick on Au electrodes showed Ohmic contacts in the 1−5 V region.[16] Studies of GaClPc suggest that electrode surface impurities can lead to Ohmic instead of SCLC behavior. If charge transport is determined by carrier injection from the electrode, it raises the question as to whether the chemical sensing properties might also depend on the electrode materials and conduction mechanism. This is an important issue for chemosensing devices based on MPc materials.

Most of the research studies on charge transport properties of MPcs have been done on micron thick films sandwiched between two parallel metal plate electrodes.[6−13,17−20] Interdigitated electrodes are more practical for chemical sensing applications, because they have larger areas exposed for analytes to diffuse into the films. Nanometer rather than micron film thicknesses are also desirable to minimize analyte diffusion/adsorption times in sensor films for rapid sensor response. However, there are only a few studies about MPc charge transport properties in a planar electrode configuration.[10,15,21] This study employs interdigitated electrodes fabricated by using photolithography with an electrode spacing of 5 μm. Nanoscale films have been deposited by OMBE under ultrahigh vacuum (UHV) and results show that the MPc−electrode interface plays a significant role in charge transport, especially at low applied voltages. The MPc−electrode interfacial region traps injected charge carriers and increases the bulk resistance. To probe the influence of the MPc−electrode interface on the transitional voltage between Ohmic and SCLC, MPc thin films were deposited by OMBE on several electrode materials.

We have also compared chemical sensitivity of MPc thin film devices on different electrode materials in both Ohmic and SCLC regimes to determine if the source of the charge carriers influences the chemical sensitivity of the films. A key question is whether analyte-induced changes at the MPc−electrode junction influence the sensor response. Maintaining a constant resistance from device to device is difficult to control, but this issue is crucial for obtaining reproducible chemical sensor responses. In particular, we investigated whether the operating conditions of the device can be manipulated to obtain consistent chemosensor responses. Most previous studies on MPc films have focused on chemical sensing of strong hole generating oxidants, such as nitrogen dioxide and ozone at high device operating temperatures (>100 °C),[10,22−31] whereas few have

---

[†] Department of Chemistry and Biochemistry.
[§] Materials Science and Engineering Program.
[‡] Department of Physics.
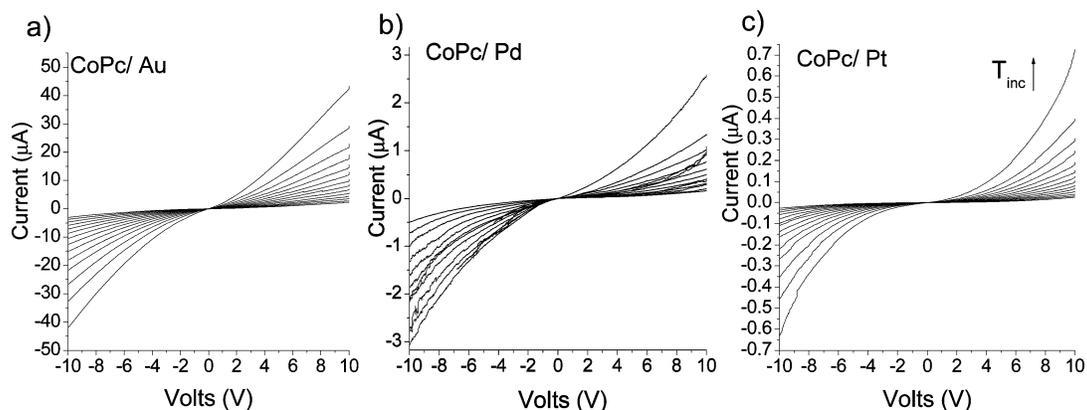[⊥] E-mail: akummel@ucsd.edu.
[∥] E-mail: wtrogler@ucsd.edu.

362 *J. Phys. Chem. B, Vol. 110, No. 1, 2006*

Miller et al.

Figure 1. *I−V* curves of CoPc on (a) Au, (b) Pd, and (c) Pt showing the temperature dependence from 278 to 343 K in 5 deg increments from the bottom to top curves as observed from the right side of each curve.

examined less reactive vapor analytes, such as DIMP (dimethylmethylphosphonate).[26,32] In the present study, the exposure of 50 nm MPc thin films at 25 °C to water and to nonreactive volatile organic vapors, such as methanol, toluene, and a nerve gas simulant, DMMP, is examined. The results demonstrate sensitive responses from the above nonreactive vapors at ambient temperature. The chemical sensing results correlate well with the charge transport studies. A practical operation strategy is proposed to minimize sensor drift and maintain uniform chemosensitivity among different devices. By operating devices under SCLC conditions, the chemosensor response becomes independent of the influence of the analyte absorption at the MPc−electrode interface causing the response to become uniform and reliable.

Experimental Section

1. Microelectrode Fabrication. A 6500 Å SiO₂ layer was thermally grown on Si(100) substrates. Interdigitated electrodes (IDEs) with 50 pairs of 10 μm wide, 5 μm spaced fingers were prepared via photolithography in a clean room. The length of fingers is 4 mm. A Ti adhesion layer of 50 Å was deposited on SiO₂ before depositing 500 Å thick Au, Pd, and Pt electrodes, using an electron-beam evaporator.

2. MPc Thin Film Deposition. Cobalt phthalocyanine (CoPc) was purchased from Aldrich and purified by zone sublimation at 400 °C and 10^{-3} to 10^{-4} Torr. Films of 500 Å thickness were evaporated from a differentially pumped hot-lip evaporation cell in an organic molecular beam epitaxy (OMBE) chamber. The OMBE chamber had a base pressure of <5 × 10^{-10} Torr and a fast introduction loadlock. The substrate temperature was kept at 300 K during deposition. The growth rate was monitored by using a water-cooled quartz crystal microbalance (QCM), which was calibrated with X-ray diffraction (XRD) and atomic force microscopy (AFM) measurements. During deposition, the chamber background pressure was around 8 × 10^{-9} Torr.

3. Current−Voltage Measurements. Contacts to the electrodes were made with use of gold pins. Devices were placed in a stainless steel sensor chamber with electrical feedthroughs and a closed-loop temperature control. The temperature could be controlled to better than ±0.1 K. Current−voltage (*I−V*) curves were measured between 343 and 278 K, using a Keithley 6517/6521 electrometer interfaced to a personal computer. The IDE devices were allowed to equilibrate at each temperature, and the voltage was scanned from +10 to −10 V in 0.1 V increments at each temperature. Several samples were checked for hysteresis and none was observed.

4. Impedance Measurements. The impedance spectroscopic studies were performed with the use of a Solartron 1260 impedance analyzer interfaced to the sample through a Solartron 1296 dielectric interface. A small amplitude AC voltage (100 mV) was applied in the frequency range of 0.1 Hz to 10 MHz.

5. Flow System for Chemical Sensing. Chemical sensing experiments were carried out in the same flow chamber used for the *I−V* measurements. The internal volume of the chamber was 15 cm³. The temperature in the chamber was kept at 298 K, using a Haake constant-temperature bath to circulate coolant through the chamber walls. Ultrahigh purity N₂ was used as both the purge and the carrier gas. A constant total flow of 500 sccm was employed for the dosing measurements. A four-way valve was used to minimize the dead time between introduction of each analyte. Bubblers filled with liquid analyte were kept in a water bath chilled to 288 K. Mass flow controllers were used to dilute and introduce vaporized analytes at a known concentration into a manifold to premix with the carrier gas before introduction into the test chamber. Solenoid valves before and after the analyte bubblers were used to prevent cross-contamination between analytes. The analytes employed were dimethyl methylphosphonate (DMMP) (a simulant for sarin), water, methanol (CH₃OH), and toluene (C₆H₅CH₃)(CH₃)(CH₃O)₂-(O)P.

Results and Discussion

1. Current−Voltage Characteristics of CoPc Thin Films. To ensure that all the devices had continuous films with good electrical contact to the electrodes, the conductivity was measured as a function of temperature. The *I−V* curves were measured between 278 and 343 K with 5 deg increments per step. All devices showed well-behaved temperature dependences; as expected for semiconducting films more current passed through the devices at higher temperatures (Figure 1).

Current−voltage studies of 50 nm thick CoPc films on Au, Pd, and Pt electrodes show a marked variation of the net device conductivity. All devices exhibit Ohmic and space-charge limited conductivity at low and high applied fields, respectively. In the SCLC region, the current density for a discrete trap distribution is given as

$$J = IA = \frac{9}{8}\epsilon\theta\mu\frac{V^2}{d^3} \tag{1}$$

where *J* is the current density, *I* is the current, *A* is the electrode area, ϵ is the permeability of the semiconductor, θ is the ratio between free and trapped charges, μ is the carrier mobility, *V* is the voltage, and *d* is the electrode spacing. To simplify the

Electrical Properties of Metallophthalocyanine Films

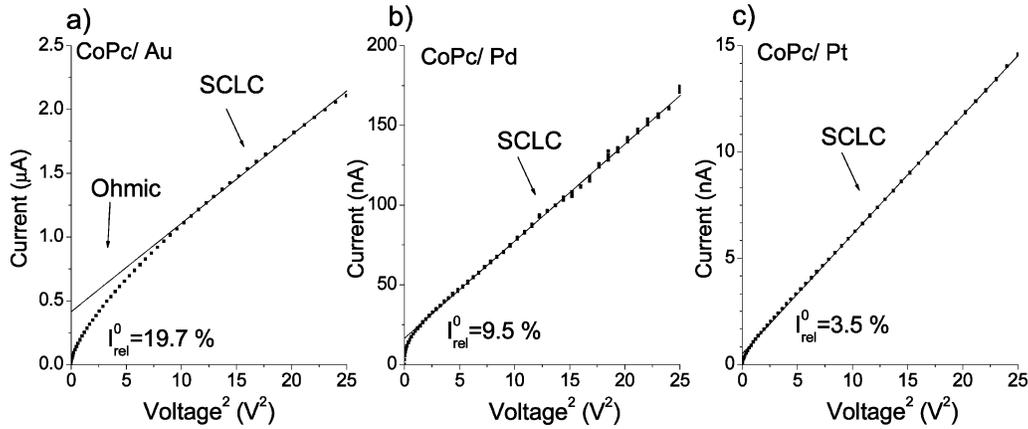*J. Phys. Chem. B, Vol. 110, No. 1, 2006* **363**

Figure 2. $I-V^2$ plots for 50 nm thick CoPc films on a Au (a), Pd (b), and Pt (c) at 298 K.

TABLE 1: Transitional Voltage between Ohmic and SCLC and the Deviation Ratio for Three 50 nm CoPc Films on Au, Pd, and Pt Interdigitated Electrodes

	CoPc/Au	CoPc/Pd	CoPc/Pt
V_T (V)	2.8	1.6	1.3
I_{rel}^0 (%)	19.7	9.5	3.5

analysis, current is plotted as a function of V^2 (see Figure 2). At high voltage, the $I-V^2$ dependence is linear and can be fitted with the above equation.

The $I-V^2$ data deviate from linearity at low voltages where Ohmic conductivity dominates. We define the deviation from linearity as $I_{rel}^0 = I_0/I_5$, to quantify the transitional behavior, where I_0 is the extrapolated current on the $I-V^2$ plot at 0 V, and I_5 is the measured current at 5 V (see Figure 2).

The transitional voltage (V_T) between the two conductivity modes was determined for each device and summarized together with the deviation ratio in Table 1. It has been found that CoPc on the Au electrode has the highest transitional voltage, while CoPc on Pt has the lowest transitional voltage. The results cannot be explained in terms of metal work function difference (Au, 5.1 eV; Pt, 6.35 eV; Pd, 5.12 eV). Because Au and Pd have a similar work function, the potential barrier for hole transport between the metal and CoPc should be the same. Since the transitional voltage of CoPc on Au is twice as large as that on Pd, this behavior must arise from some other factor, such as the structural difference of the interfacial layer between CoPc and the various metal electrodes. A 300× difference in conductivity is observed for the different devices, even though all devices contain the same thickness of CoPc. This further illustrates the importance of the interfacial layer on the device charge transport response. In pentacene thin film transistors, the small grain size of the organic material at the edge of the electrode contact has been linked to the creation of charge carrier traps and reduced conductivity.[33]

2. Impedance Spectroscopic Study of CoPc Thin Films. Impedance spectroscopy uses variable-frequency AC signals to simultaneously measure the frequency dependent resistance and capacitance. The studies can reveal the coexistence of low- and high-frequency traps in the CoPc thin films, which may result from interfacial vs bulk charge traps. The results from these studies correlate well with the current−voltage measurements.

The impedance of a device can be expressed as in eq 2:

$$Z(\omega) = Z'(\omega) + jZ''(\omega) = R(\omega) - j\frac{1}{\omega C(\omega)}, j = i = \sqrt{-1}$$
(2)

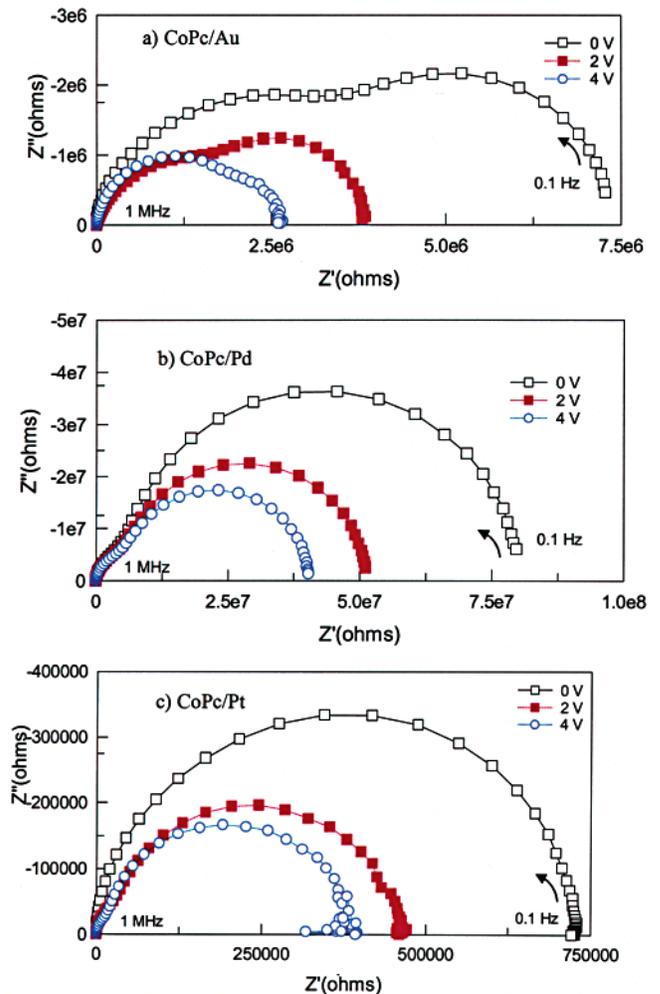where Z' and Z'' are the real and imaginary parts of impedance,

Figure 3. Plots of the complex impedance plane responses of (a, top) CoPc/Au, (b) CoPc/Pd, and (c) CoPc/Pt 5 μm IDE devices.

which represent resistive and capacitive components in the device, and $\omega = 2\pi f$ is the angular frequency. Shown in Figure 3 are the impedance spectra of CoPc/Au, CoPc/Pd, and CoPc/Pt devices plotted in the complex plane. The frequency increases from right to left, from 0.1 Hz to 1 MHz. For a circuit with an ideal resistor and capacitor in parallel, one perfect semicircle should be observed in the complex plane. The RC relaxation time τ can be determined when the magnitudes of real and imaginary parts are equal,

$$Z' = Z''$$

$$\tau = \frac{1}{\omega} = RC \qquad (3)$$

In real organic devices, the semicircles are often distorted due to a distribution of relaxation times. If the relaxation times differ by more than 2 orders of magnitude, then two semicircles can be observed instead of one.[34−38] For example, two semicircles are clearly resolved in the CoPc/Au device shown in Figure 3a. The low-frequency semicircle is attributed to interfacial traps because such traps typically have longer relaxation lifetimes.[39] The high-frequency semicircle is attributed to bulk traps because bulk materials are typically more ordered than the interface, and therefore have faster charge relaxation. In the CoPc/Pt device, only one semicircle is found, which suggests that charge transport is dominated by the bulk material. This is also consistent with DC conductivity measurements (Figure 2), which show that SCLC behavior is dominant for the Pt electrode device. In the CoPc/Pd device, an intermediate behavior was found, and there are two semicircles in the impedance spectrum of Figure 3b. Since the relaxation time constants do not differ by at least 2 orders of magnitudes, only distorted semicircles are observed.

The coexistence of interface and bulk traps is further documented by DC voltage dependence impedance experiments. At the interface between organic semiconductors and metals, localized electronic states may trap significant amounts of charge, which act as potential barriers for carrier transport. With an applied DC bias, the interface traps are turned into fixed charges and do not follow the AC signals impedance measurements.[40] As shown in Figure 3a, the low-frequency semicircle diminishes with increasing bias. These experiments suggest that the observed Ohmic behavior (Figure 2) at low voltages in CoPc/Au arises because the injected carriers from the electrodes are trapped at the interface. At high voltages, when these traps are filled, SCLC behavior is observed.

3. Proposed Growth Models. It has been realized that the bulk, surface, and contact layers of organic thin films play a significant role in MPc sensors.[41] Figure 4 shows a proposed model for the three distinct interfaces present in the IDE devices: CoPc deposited on SiO$_2$, CoPc deposited on metal electrodes, and the interface between the CoPc−SiO$_2$ and the CoPc−metal growth fronts. According to the studies of MPc growth on polycrystalline metals and thermal oxides, the MPc molecules tend to stand on edge (oriented near 90° relative to the SiO$_2$ and metal surfaces) on the substrate as the molecule−substrate interactions are weaker than molecule−molecule interactions.[40,42] Since the electrode height (50 nm) will not precisely exceed that of the nominally 50 nm MPc layer, the junction of the two growth fronts is expected to be disordered.

Since the SiO$_2$ surface is the same for all the devices, this interface cannot account for the differences in conductivity observed for a given CoPc of the different electrode materials. Therefore, the difference in the magnitude of conductivity and transition voltage between Ohmic and SCLC behavior must be due to either the different growth of the MPc on the metal electrodes or the interface between the two MPc growth fronts. Both of these might play a critical role in chemical sensing. Since analytes interact with the MPc molecules in the bulk as well as at the interface, a source of sensor drift and irreproducibility could be analyte interactions at the MPc electrode and growth front interfaces. Chemical sensing studies were performed to test if high-voltage operation eliminated the dependence of the electrical properties of the devices from analyte interactions at the electrode−MPc interface, while
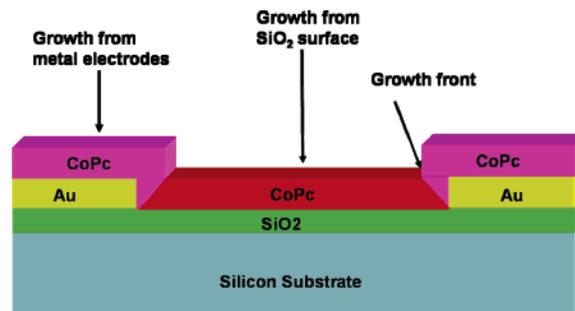

Figure 4. Proposed growth model of CoPc on interdigitated electrodes, which depicts the expected difference in ordered growth on metal vs SiO$_2$.

retaining the dependence of the electrical properties on the interaction of the analytes with the bulk of the MPc film.

4. The Effect of Chemical Sensing Response. The same devices used in the conductivity studies were tested as chemosensors at room temperature and exposed to four different analytes. The use of 50 nm thick MPc sensor films provides reasonable current response and reversibility to analyte exposure on the order of minutes (Figure 5) at room temperature. While the initially prepared sensors show significant baseline drift, several annealing cycles at 50 °C produce sensors that show good baseline stability (Figure 5). There were not gross differences in surface grain structure (determined by AFM) after annealing. The I−V characteristics of annealed samples do not differ significantly in the voltage range observed for Ohmic and SCLC behavior.

Varying the electrode material results in over a 300× difference in conductivity for the different devices. However, at 5 V, where SCLC behavior dominates, the devices all show (Table 3) the same relative response (within 5%) toward analytes, such as DMMP, water, methanol, and toluene (Table 2). Such independence, regardless of the overall conductivity, suggests that the analyte and MPc film interact by the same mechanism, independent of differences in the electrode−MPc or growth front interfaces. Since most of the MPc film lies between the metal electrodes, it seems reasonable that this large adsorbing region of MPc dominates the chemical sensor response. The relative response toward analytes does not depend on the CoPc−metal interface at high voltage where SCLC dominates, which suggests that the interfacial traps are turned into fixed charge as the bias increases, preventing their contribution to the chemical sensing response.

From device to device, MPc−metal electrode interfacial layers may have larger variation than the bulk film and a greater tendency to change over time as the electrode corrodes, or as the interfacial strain between the dissimilar materials relaxes. To test the above hypothesis, similar experiments were carried out in the Ohmic regime for the three devices. The relative chemical sensitivity data are tabulated in Table 3. It has been found the variation in chemical sensor response among devices can be as high as 26% in the case of DMMP, which is 10 times higher than the variation observed when the device is operated in the SCLC regime. This finding suggests that resistive MPc chemical sensors should be operated in the SCLC regime to minimize the influence of interfacial variations on the device's chemosensor response.

Conclusions

The DC conductivity of CoPc on different metal interdigitated electrodes (IDE) exhibits Ohmic conductivity at low applied potentials and space-charge limited conductivity at higher
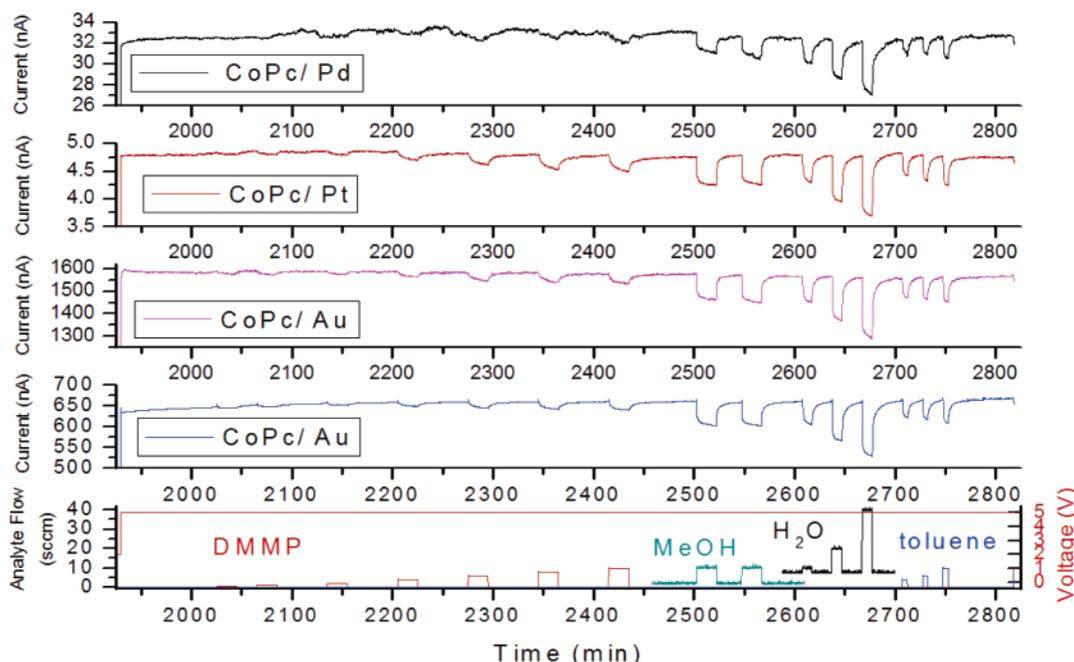
Electrical Properties of Metallophthalocyanine Films

J. Phys. Chem. B, Vol. 110, No. 1, 2006 **365**

Figure 5. Current response of CoPc devices for DMMP, methanol, water, and toluene for 5 V applied across the electrodes. The bottom panel shows the dosing sequence, the other panels show the device response.

TABLE 2: Relative Sensitivities at 5 V Normalized to That of a 5% Relative Humidity (RH) Change for Devices Tested, Plotted as the Ratio of $I_{analyte}/I_{H_2O}$

	DMMP (100 ppm)	MeOH (1900 ppm)	H_2O (5% Δ RH)	toluene (400 ppm)
CoPc/Pd	1.19	1.15	1	1.13
CoPc/Pt	1.22	1.15	1	1.15
CoPc/Au	1.19	1.13	1	1.13
CoPc/Au	1.20	1.13	1	1.14

TABLE 3: Relative Sensitivities at 1 V Normalized to That of a 6% Relative Humidity (RH) Change for Devices Tested, Plotted as the Ratio of $I_{analyte}/I_{H_2O}$

	DMMP (100 ppm)	MeOH (1900 ppm)	H_2O (6% Δ RH)	toluene (400 ppm)
CoPc/Pd	1.17	1.13	1	1.11
CoPc/Pt	1.48	1.29	1	1.23
CoPc/Au	1.28	1.18	1	1.18
CoPc/Au	1.36	1.24	1	1.19

applied potentials. Some electrodes show mostly SCLC behavior between 1 and 10 V. These differences in conductivity mechanism arise from the role of MPc−electrode interface, in addition to the growth front interfaces between MPc−electrode growth and MPc−SiO$_2$ growth. At low applied voltages, a large portion of the injected carriers are immobilized by interfacial traps and hence Ohmic conductivity is observed. At higher applied potentials, these interface trap sites are filled, and therefore, SCLC is observed. Even in the SCLC region, over a 300× variation in bulk conductivity is observed. The results indicate that the transition voltage between Ohmic and SCLC, as well as the net conductivity of a device, depends strongly on the interface between MPc and metal electrodes.

Despite these large MPc−electrode interfacial effects on device conductivity, the chemical sensor response ($\Delta I/I_{baseline}$) toward various analytes in the SCLC region is not affected by the metal electrode employed. It is concluded that the bulk film is responsible for chemical sensing when the device is operated within the SCLC regime. Because the low-frequency interfacial traps are filled in the SCLC region, the sensor response becomes independent of the influence of the analyte absorption at the

MPc−electrode interface and the analyte response is independent of electrode material. The use of thin film samples prepared by OMBE permits the fabrication of metallophthalocyanine sensors that operate at ambient temperature.

References and Notes

(1) *Phthalocyanines Properties and Applications*; Leznoff, C. C., Lever, A. B. P., Eds.; John Wiley & Sons: New York, 1989; Vol. 1.
(2) Schmidt, A.; Chau, L. K.; Back, A.; Armstrong, N. R. *Phthalocyanines* **1996**, *4*, 307.
(3) Armstrong, N. R. *J. Porphyrins Phthalocyanines* **2000**, *4*, 414.
(4) Hung, L. S.; Tang, C. W. *Appl. Phys. Lett.* **1999**, *74*, 3209.
(5) Bao, Z.; Lovinger, A. J.; Dodabalapur, A. *Appl. Phys. Lett.* **1996**, *69*, 3066.
(6) Abdel Malik, T. G.; Abdel-Latif, R. M. *Thin Solid Films* **1997**, *305*, 336.
(7) Gould, R. D. *J. Appl. Phys.* **1982**, *53*, 3353.
(8) Gould, R. D. *J. Phys. D: Appl. Phys.* **1986**, 1785.
(9) Gould, R. D. *Coord. Chem. Rev.* **1996**, *156*, 237.
(10) Gould, R. D.; Ibrahim, N. A. *Thin Solid Films* **2001**, *398−399*, 432.
(11) Gould, R. D.; Shafai, T. S. *Thin Solid Films* **2000**, *373*, 89.
(12) Hassan, A. K.; Gould, R. D. *Int. J. Electron.* **1992**, *73*, 1047.
(13) Saleh, A. M.; Hassan, A. K.; Gould, R. D. *J. Phys. Chem. Solids* **2003**, *64*, 1297.
(14) Hiller, S.; Schlettwein, D.; Armstrong, N. R.; Wohrle, D. *J. Mater. Chem.* **1998**, *8*, 945.
(15) Pankow, J. W.; Arbour, C.; Dodelet, J. P.; Collins, G. E.; Armstrong, N. R. *J. Phys. Chem.* **1993**, *97*, 8485.
(16) Blochwitz, J.; Fritz, T.; Pfeiffer, M.; Leo, K.; Alloway, D. M.; Lee, P. A.; Armstrong, N. R. *Org. Electron.* **2001**, *2*, 97.
(17) Hassan, A. K.; Gould, R. D. *J. Phys.: Condens. Matter* **1989**, *1*, 6679.
(18) Inabe, T.; Tajima, H. *Chem. Rev.* **2004**, *104*, 5503.
(19) Inabe, T. *J. Porphyrins Phthalocyanines* **2001**, *5*, 3.
(20) El Beqqali, O.; Al Sadoun, M.; Guillaud, G.; Gamoudi, M.; Benkaddour, M.; Skal, A. S.; Maitrot, M. *J. Appl. Phys.* **1991**, *69*, 3670.
(21) Zhou, Q.; Gould, R. D. *Thin Solid Films* **1998**, *317*, 432.
(22) Bott, B.; Jones, T. A. *Sens. Actuators* **1984**, *5*, 43.
(23) Bouvet, M.; Guillaud, G.; Leroy, A.; Maillard, A.; Spirkovitch, S.; Tournilhac, F.-G. *Sens. Actuators, B* **2001**, *73*, 63.
(24) Guillaud, G.; Simon, J.; Germain, J. P. *Coord. Chem. Rev.* **1998**, *178−180*, 1433.
(25) Hsieh, J. C.; Liu, C. J.; Ju, Y. H. *Thin Solid Films* **1998**, *322*, 98.

(26) Kolesar, E. S., Jr.; Wiseman, J., M. *Anal. Chem.* **1989**, *61*, 2355.

(27) Snow, A. W.; Barger, W. R. Phthalocyanine Films in Chemical Sensors. In *Phthalocyanines Properties and Applications*; Lever, A. B. P., Ed.; John Wiley & Sons: New York, 1989; Vol. 1, p 341.

(28) Lever, A. B. P. *J. Porphyrins Phthalocyanines* **1999**, *3*, 488.

(29) Wright, J. D. *Prog. Surf. Sci.* **1989**, *31*, 1.

(30) Zhou, R.; Josse, F.; Gopel, W.; Oeztuerk, Z. Z.; Bekaroglu, O. *Appl. Organomet. Chem.* **1996**, *10*, 557.

(31) Barger, W. R.; Wohltjen, H.; Snow, A. W.; Lint, J.; Jarvis, N. L. *ACS Symp. Ser.* **1986**, *309*, 155.

(32) Grate, J. W.; Klusty, M.; Barger, W. R.; Snow, A. W. *Anal. Chem.* **1990**, *62*, 1927.

(33) Dimitrakopoulos, C. D.; Mascaro, D. J. *IBM J. Res. Dev.* **2001**, *45*, 11.

(34) MacDonald, J. R. *Impedance Spectroscopy*; John Wiley and Sons: New York, 1987.

(35) Eder, D.; Kramer, R. *J. Phys. Chem. B* **2004**, *108*, 14823.

(36) Endres, E.; Drost, S.; Hutter, F. *Sens. Actuators, B* **1994**, *22*, 7.

(37) Hogan, J.; Brinkman, A. W.; Hashemi, T. *Appl. Phys. Lett.* **1998**, *202*, 3077.

(38) Kurzweil, P.; Maunz, W.; Plog, C. *Sens. Actuators, B* **1995**, *25*, 653.

(39) Gutierrez, J.; Ares, L.; Horillo, M. C.; Sayago, I.; Agapito, J.; Lopez, L. *Sens. Actuators, B* **1991**, *4*, 359.

(40) Knupfer, M.; Peisert, H. *Phys. Status Solidi A* **2004**, *201*, 1055.

(41) Janata, J. *Phys. Chem. Chem. Phys.* **2003**, *5*, 5155.

(42) Miller, C. W.; Sharoni, A.; Liu, G.; Colesniuc, C. N.; Fruhberger, B.; Schuller, I. K. Submitted for publication.